THE ASTRONOMICAL JOURNAL, 146:100 (12pp), 2013 October doi:10.1088/0004-6256/146/4/100

DISCOVERING BRIGHT QUASARS AT INTERMEDIATE REDSHIFTS BASED ON OPTICAL/NEAR-INFRARED COLORS

XUE-BING WU, WENWEN ZUO, JINYI YANG, QIAN YANG, AND FEIGE WANG
Department of Astronomy, Peking University, Beijing 100871, China; wuxb@pku.edu.cn
Received 2012 July 1; accepted 2013 August 6; published 2013 September 13

ABSTRACT

The identification of quasars at intermediate redshifts ($2.2 < z < 3.5$) has been inefficient in most previous quasar surveys since the optical colors of quasars are similar to those of stars. The near-IR K-band excess technique has been suggested to overcome this difficulty. Our recent study also proposed to use optical/near-IR colors for selecting $z < 4$ quasars. To verify the effectiveness of this method, we selected a list of 105 unidentified bright targets with $i \leqslant 18.5$ from the quasar candidates of SDSS DR6 with both SDSS *ugriz* optical and UKIDSS *YJHK* near-IR photometric data, which satisfy our proposed $Y - K/g - z$ criterion and have photometric redshifts between 2.2 and 3.5 estimated from the nine-band SDSS-UKIDSS data. We observed 43 targets with the BFOSC instrument on the 2.16 m optical telescope at Xinglong station of the National Astronomical Observatory of China in the spring of 2012. We spectroscopically identified 36 targets as quasars with redshifts between 2.1 and 3.4. The high success rate of discovering these quasars in the SDSS spectroscopic surveyed area further demonstrates the robustness of both the $Y - K/g - z$ selection criterion and the photometric redshift estimation technique. We also used the above criterion to investigate the possible stellar contamination rate among the quasar candidates of SDSS DR6, and found that the rate is much higher when selecting $3 < z < 3.5$ quasar candidates than when selecting lower redshift candidates ($z < 2.2$). The significant improvement in the photometric redshift estimation when using the nine-band SDSS-UKIDSS data over the five-band SDSS data is demonstrated and a catalog of 7727 unidentified quasar candidates in SDSS DR6 selected with optical/near-IR colors and having photometric redshifts between 2.2 and 3.5 is provided. We also tested the $Y - K/g - z$ selection criterion with the recently released SDSS-III/DR9 quasar catalog and found that 96.2% of 17,999 DR9 quasars with UKIDSS Y- and K-band data satisfy our criterion. With some available samples of red quasars and type II quasars, we find that 88% and 96.5% of these objects can be selected by the $Y - K/g - z$ criterion, respectively, which supports our claim that using the $Y - K/g - z$ criterion efficiently selects both unobscured and obscured quasars. We discuss the implications of our results on the ongoing and upcoming large optical and near-IR sky surveys.

Key words: galaxies: active – galaxies: high-redshift – quasars: emission lines – quasars: general

Online-only material: color figures, machine-readable and VO tables

1. INTRODUCTION

Quasars are important extragalactic objects in astrophysics due to their unusual properties. Not only can they be used to probe the physics of supermassive black holes and accretion/jet processes, but quasars are also closely related to studies of galaxy evolution, the intergalactic medium, large scale structure, and cosmology. The number of observed quasars has increased steadily since their discovery in 1963 (Schmidt 1963; Hazard et al. 1963; Oke 1963; Greenstein & Matthews 1963). In particular, a large number of quasars have been discovered in the last two decades in two large spectroscopic surveys, namely the Two-Degree Fields (2DF) quasar survey (Boyle et al. 2000) and the Sloan Digital Sky Survey (SDSS; York et al. 2000). 2DF mainly selected low redshift ($z < 2.2$) quasar candidates with UV excesses (Smith et al. 2005) and has discovered more than 20,000 blue quasars (Croom et al. 2004), while SDSS adopted a multi-band optical color selection method (Richards et al. 2002) and has identified more than 120,000 quasars (Schneider et al. 2010). 90% of SDSS quasars are at low redshifts ($z < 2.2$), although some dedicated methods were also proposed for finding high-redshift quasars ($z > 3.5$; Fan et al. 2001a, 2001b; Richards et al. 2002).

However, in the redshift range $2.2 < z < 3.5$, the selection of SDSS quasars is inefficient. Richards et al. (2006) demonstrated this problem by checking the efficiency of SDSS quasar selection with the FIRST radio quasars and found that the efficiency drops substantially in the redshift range $2.2 < z < 3.5$. There are two remarkable dips, one around $z = 2.8$ and another around $z = 3.4$. The reason for this problem is well understood. At redshifts $2.2 < z < 3.5$, the spectral energy distributions of quasars show similar optical colors to those of normal stars and quasar selection using optical color–color diagrams becomes very inefficient due to the serious stellar contamination (Fan 1999; Richards et al. 2002, 2006; Schneider et al. 2007; Hennawi et al. 2010). In addition, SDSS preferentially selects $3 < z < 3.5$ quasars with intervening H I Lyman limit systems, which can also result in a lower efficiency in identifying quasars with redshifts around $z = 3.4$ (Worseck & Prochaska 2011). Because of the importance of using the Lyα forest of $z > 2.2$ quasars to study cosmic baryon acoustic oscillations (BAOs; White 2003; McDonald & Eisenstein 2007) and relying on quasars to construct an accurate luminosity function to study quasar evolution in the mid-redshift universe (Wolf et al. 2003; Jiang et al. 2006), we need to explore other more efficient ways of identifying $2.2 < z < 3.5$ quasars than using optical colors alone. We note that significant efforts have been made recently in terms of quasar target selection in the SDSS-III Baryon Oscillation Spectroscopic Survey (BOSS; Eisenstein et al. 2011; Ross et al. 2012), and many more quasars at intermediate redshifts have been found in SDSS-III/DR 9 (Paris et al. 2012).

One possible way to identify $2.2 < z < 3.5$ quasars is to use optical variability, as variability is a well known quasar property (Hook et al. 1994; Cristiani et al. 1996; Giveon et al. 1999). Selecting quasars based on variability is usually thought to be less biased than techniques based on optical colors, although more variation at shorter wavelengths has been found for SDSS quasars (Vanden Berk et al. 2004; Zuo et al. 2012). Recently, Schmidt et al. (2010), MacLeod et al. (2011), and Butler & Bloom (2011) proposed to select quasar candidates by constructing various intrinsic variability parameters from the light curves of known quasars in SDSS Stripe 82 (hereafter S82; see also Sesar et al. 2007). They claimed that with their methods they can efficiently separate quasars from stars and can substantially increase the number of known quasars at $2.5 < z < 3.0$. Moreover, recent results from SDSS-III/BOSS (Eisenstein et al. 2011) also confirmed the high success rate of spectroscopically identifying variability selected quasars, which leads to a significant increase in the $z > 2.2$ quasar density in S82 over that based on optical color-selected quasars (Palanque-Delabrouille et al. 2011; Ross et al. 2012). However, only for very limited sky areas have the multi-epoch observational data been made publicly available, so at the present time variability methods cannot be broadly used for selecting quasars over a large sky area.

Another possible way for separating $z > 2.2$ quasars from stars is to utilize the near-IR colors of quasars. Due to the different radiative mechanisms of stars and quasars, the continuum emission from stars usually has a blackbody-like spectrum and decreases more rapidly from the optical to near-IR wavelengths than do the spectra of quasars, which usually display a power-law behavior over a broad range of wavelength plus thermal emission from accretion disks and dust. This fact leads to obvious color differences between stars and quasars in near-IR bands, even though their optical spectra are similar. Because of this difference, a K-band excess technique has been proposed for identifying quasars at $z > 2.2$ (e.g., Warren et al. 2000; Croom et al. 2001; Sharp et al. 2002; Hewett et al. 2006; Chiu et al. 2007; Maddox et al. 2008, 2012; Smail et al. 2008; Wu & Jia 2010). Based on a sample of 8498 quasars and a sample of 8996 stars complied from the photometric data in the *ugriz* bands of SDSS and the *YJHK* bands of the UKIRT InfraRed Deep Sky Surveys (UKIDSS[1]), Wu & Jia (2010) proposed an efficient empirical criterion, (i.e., $Y - K > 0.46(g - z) + 0.82$, where $Y - K$ magnitudes are Vega magnitudes and $g - z$ magnitudes are AB magnitudes) for selecting $z < 4$ quasars. A check with the VLA-FIRST (Becker et al. 1995) radio-detected SDSS quasars, which are thought to be free of color selection bias (see McGreer et al. 2009, however), also proved that with this $Y - K/g - z$ criterion they can achieve a completeness higher than 95% for these radio-detected quasars at $z < 3.5$, which seems to be difficult when using the SDSS optical color selection criteria alone; the SDSS criteria produce two dips around $z \sim 2.7$ and $z \sim 3.4$ (Richards et al. 2002, 2006; Schneider et al. 2007, 2010). Recently, Peth et al. (2011) extended the study of Wu & Jia (2010) to a larger sample of 130,000 SDSS-UKIDSS-selected quasar candidates and re-examined their near-IR/optical colors.

Although by combining variability and optical/near-IR colors we can achieve the maximum efficiency in identifying $2.2 < z < 3.5$ quasars (Wu et al. 2011), for most sky areas we still lack publicly available variability data. One may also think of using radio and X-ray data, but these data can only be helpful for selecting specific quasar samples (White et al. 2000; Green et al. 1995), which represent only a small fraction of the whole quasar population. Therefore, using optical/near-IR colors is probably still the most important way of selecting $2.2 < z < 3.5$ quasars. Although we have made some observations to identify a few $z > 2.2$ quasars (Wu et al. 2010a, 2010b, 2011), more efforts are still needed to check whether using our $Y - K/g - z$ criterion can help us to discover more quasars at $2.2 < z < 3.5$, especially in the SDSS spectroscopically surveyed area.

This paper is organized as follows. In Section 2, we will describe the target selections and spectroscopic observations and report our discovery of 36 new $2.2 < z < 3.5$ quasars. In Section 3, we use our $Y - K/g - z$ criterion to check the possible contaminations of stars in the quasar candidate catalog of SDSS DR6 and investigate the improvement in the photometric redshift estimation using the nine-band SDSS-UKIDSS data. In Section 4, we check the effectiveness of our $Y - K/g - z$ criterion in selecting quasars with the recently released SDSS-III/DR9 quasar catalog. In Section 5, we check whether we can use the $Y - K/g - z$ criterion to select red quasars and type II quasars. In Section 6, we estimate how many $2.2 < z < 3.5$ quasars we can select in additional to the SDSS-III/BOSS quasars. Finally, we discuss our results and their implications in Section 7.

2. TARGET SELECTION AND SPECTROSCOPIC OBSERVATIONS

2.1. Target Selection

The main purpose of our study is to use our proposed $Y - K/g - z$ criterion to discover more quasars at $2.2 < z < 3.5$ in the SDSS spectroscopically surveyed area. We started from the 1 million quasar candidates in SDSS DR6 given by Richards et al. (2009, hereafter R09) from Bayesian classification and selected 8845 unidentified quasar candidates brighter than $i = 18.5$. From these objects, we further selected 2149 candidates with photometric redshifts greater than 2.2 in R09 and a redshift probability higher than 0.5. Then, we cross-matched these quasar candidates with the UKIDSS/Large Area Survey (LAS) DR7 using a positional offset within $3''$ and recovered 401 candidates with both SDSS *ugriz* and UKIDSS *YJHK* photometric data. 126 of these objects satisfy our $Y - K > 0.46(g - z) + 0.82$ criterion for selecting $z < 4$ quasars (Wu & Jia 2010). 17 out of these 126 candidates have been spectroscopically identified as quasars after the SDSS DR6, and 15 of them have redshifts greater than 2.2. Another candidate was identified as a white dwarf. After excluding these 18 known objects, we obtained a list of 108 quasar candidates.

Since these quasar candidates have nine-band SDSS and UKIDSS photometric data, the photometric redshifts obtained from these nine-band data are more accurate than those given by the five-band SDSS photometric data (Wu & Jia 2010). We use our developed program to estimate photometric redshifts based on the nine-band data and found that 15 objects out of 108 quasar candidates have photometric redshifts smaller than 2, while for other quasar candidates our results are consistent with those obtained in R09 from the SDSS photometric data. After excluding these 15 objects, we obtain a target list of 93 quasar candidates with reliable photometric redshifts between 2.2 and 3.6. After the public release of UKIDSS/LAS DR8 in 2012 April, we also added other 12 quasar candidates that have UKIDSS/LAS DR8 data and satisfy our $Y - K/g - z$ selection criterion but were not included in the UKIDSS/LAS DR7,

[1] The UKIDSS project is defined in Lawrence et al. (2007). UKIDSS uses the UKIRT Wide Field Camera (Casali et al. 2007) and a photometric system described in Hewett et al. (2006). The pipeline processing and science archive are described in Hambly et al. (2008).

Table 1
Procedures of Target Selection

Step	Number of Candidates	Description
1	1,015,082	All quasar candidates in R09
2	925,899	Excluding known quasars in SDSS DR6
3	8,845	Brighter than $i = 18.5$
4	2,149	Photometric redshift $z_{\rm phot} > 2.2$ and probability $z_{\rm prob} > 0.5$ in R09
5	401	With UKIDSS LAS DR7 data
6	126	Satisfying $Y - K > 0.46(g - z) + 0.82$ selection criterion
7	108	Excluding 17 quasars and one white dwarf identified after SDSS DR6
8	93	Excluding 15 candidates with SDSS-UKIDSS based photometric redshifts smaller than 2
9	105	Adding 12 candidates not included in UKIDSS/LAS DR7 but included in UKIDSS/LAS DR8

including in our final list 105 quasar candidates. The procedures of our target selections are also listed in Table 1.

2.2. Spectroscopic Observations

Among these 105 quasar candidates, 92 have a right ascension (R.A.) between 7hr and 17hr. In March to May of 2012, we made spectroscopic observations over eight nights of 43 bright quasar candidates (a sampling rate of 46.7%) with photometric redshifts at $2.2 < z_{ph} < 3.5$ using the BAO Faint Object Spectrograph and Camera (BFOSC) of the 2.16 m optical telescope at the Xinglong station of the National Astronomical Observatories, Chinese Academy of Sciences (NAOC). A low resolution grism with the dispersion of 198 Å/mm, wavelength coverage from 3850 to 7000 Å, and a spectral resolution of 2.97 Å was used. During our observations, the typical seeing varied from 1″.5 to 2″.5, so we accordingly adopted a long slit width of 1″.8 and 3″.6 (there was no choice in between). In Table 2, we summarize the parameters and details of the observations for these 43 quasar candidates, including the observation date, exposure time, SDSS and UKIDSS magnitudes, photometric redshift, identification result, and spectral redshift.

Among the 43 quasar candidates, 36 were spectroscopically identified as quasars with redshifts from 2.1 to 3.4, two were identified as stars, and five remain unidentified due to the lower signal-to-noise ratios (S/Ns) of their spectra. The spectra of 36 new quasars, after the standard flat-field corrections, flux calibrations, and wavelength calibrations, are plotted in Figure 1.

The spectra of these quasars were analyzed following the method described in detail in Shen et al. (2008) and Shen & Liu (2012). First, the spectra were redshift corrected to the rest frame and corrected for Galactic extinction using the extinction map of Schlegel et al. (1998). They are then fit based on the IDL code MPFIT (Markwardt 2009). We fit the spectra with the pseudo-continuum model consisting of a featureless non-stellar continuum and Fe II emission. The featureless non-stellar continuum is assumed to be a power law, so two free parameters (the amplitude and the slope) are required. Templates for the Fe II emission were constructed from the spectrum of the narrow-line Seyfert 1 galaxy, I Zw I (Boroson & Green 1992), by convolving the spectrum with a velocity dispersion and shifting with a velocity. We used the UV template generated by Vestergaard & Wilkes (2001) and Tsuzuki et al. (2006) in the wavelength range of 1000–3500 Å.

After constructing the pseudo-continuum, the broad C IV component was fit with two Gaussians and the narrow component was fit with one Gaussian. However, as the spectra of 13 quasars have low S/Ns (∼6.5), we used only one Gaussian to fit the entire C IV emission line profile for these objects. We measured the FWHM of the C IV line (FWHM(C IV)) and the luminosity at 1350 Å (L_{1350}) from the spectra. We note that the line widths for the 13 quasars with lower S/Ns are rough estimates. The black hole mass is calculated based on FWHM(C IV) and L_{1350} using Equation (7) in Vestergaard & Peterson (2006; see also Kong et al. 2006). Using a scaling relation between L_{1350} and bolometric luminosity $L_{\rm bol}$, $L_{\rm bol} = 4.62\, L_{1350}$, we estimate the bolometric luminosity of these quasars. Based on the black hole mass and bolometric luminosity obtained, we also calculate their Eddington ratios ($L_{\rm bol}/L_{\rm Edd}$, where $L_{\rm Edd}$ is the Eddington luminosity). The results are summarized in Table 3. Although we noticed that the uncertainties of these values are probably quite large due to the low spectral quality and the unusual properties of C IV, the overall properties of these quasars, including the line width, continuum luminosity, black hole mass, and Eddington ratio, are consistent with those of typical SDSS quasars with redshifts greater than 2.2 (Shen et al. 2011). The continuum slope parameter, α_λ, is given for each quasar in Table 3. The median value of α_λ is −1.315. If we convert this value to α_ν, the median value of α_ν is then −0.685, which is not too different from the value of −0.517 and −0.862 obtained for SDSS DR9 and DR7 quasars, respectively (Paris et al. 2012).

We also investigate the broad absorption line quasars (BALs) in our sample. The balnicity index (BI) is calculated for each quasar using the traditional method (Weymann et al. 1991). 14 quasars have positive BI values, indicating that they are probably BAL quasars. However, by visually inspecting the quasar spectra, we find that this traditional method risks identifying false troughs from noisy and poor continuum fitting. To avoid these false identifications, we calculate the BI and absorption index, adding the same extra minimum depth and width requirement in the emission-line region (for more details, see Section 4.4 of Trump et al. 2006). With these procedures, we found four BALs. However, SDSS J124605.36+071128.2 is likely not a real BAL due to the lack of a spectrum shortward of the C IV line center. The remaining three BALs are SDSS J115531.45−014611.9, SDSS J1359420+022426.0, and SDSS J142405.57+044105.5. Their BI values are 3379.27, 381.18, and 178.70 km s^{-1}, respectively. The high velocities (3837–21293 km s^{-1}) derived from the broad absorption features of their C IV lines are consistent with those of quasars with higher UV luminosities (Gibson et al. 2009). This result is also expected if the BAL outflow is produced by strong radiation pressure (Murray et al. 1995).

2.3. The Success Rate of Finding 2.2 < z < 3.5 Quasars

Our spectroscopic observations identified 36 quasars at $2.1 < z < 3.4$ and two stars from 43 candidates, which indicates a success rate of at least 83.7% for identifying bright quasars at intermediate redshifts because five candidates still remain

Table 2
Parameters and Observation Details of 43 Quasar Candidates

Name (SDSS J)	Date	Exposure (s)	u	g	r	i	z	Y	J	H	K	$z_{ph}(R09)$	z_{ph}	Result	z_{sp}
075746.08+232054.2	2012 Mar 13	3600	19.06	18.46	18.48	18.47	18.27	17.69	17.39	16.82	16.02	2.365	2.375	quasar	2.532
081545.72+264847.1	2012 Apr 14	1800	18.27	17.14	17.06	17.04	16.87	16.24	15.86	15.5	15.29	2.755	2.825	F star	
081617.55+225604.5	2012 May 15	2400	19.95	18.63	18.43	18.35	18.35	17.74	17.37	16.92	16.57	2.905	2.875	quasar	2.931
083255.70+004710.1	2012 Mar 13	3600	19.80	18.40	18.29	18.30	18.28	17.89	17.36	16.92	16.54	2.905	2.875	quasar	2.919
084659.42+253940.9	2012 Apr 16	3600	19.75	18.44	18.46	18.43	18.25	17.46	17.03	16.53	15.99	2.795	2.875	quasar	2.892
085152.98+091808.5	2012 May 16	3600	18.65	18.13	17.95	17.94	17.79	17.15	16.95	16.54	15.85	2.505	2.575	low S/N	
085825.51+283258.5	2012 Mar 13	3600	20.54	18.73	18.44	18.50	18.49	17.68	17.20	16.74	16.15	3.535	2.975	quasar	3.226
090233.19+034131.2	2012 May 17	3600	18.49	17.92	17.79	17.77	17.6	17.06	16.88	16.39	15.63	2.465	2.575	quasar	2.532
090827.71+011322.5	2012 Apr 15	2400	18.33	17.64	17.54	17.47	17.29	16.83	16.51	16.07	15.26	2.565	2.325	quasar	2.083
091756.58+100836.7	2012 Apr 16	2400	18.54	17.72	17.68	17.67	17.58	16.9	16.55	16.1	15.67	2.695	2.675	quasar	2.760
091857.36+025205.4	2012 Apr 15	3000	19.39	17.9	17.79	17.72	17.61	17.06	16.75	16.39	15.9	2.905	2.875	quasar	2.789
092021.02−020113.7	2012 Mar 14	3600	19.96	18.58	18.51	18.46	18.44	17.76	17.45	17.15	16.71	2.905	2.875	quasar	2.826
093655.11+305855.3	2012 May 17	2700	20.37	18.55	18.45	18.49	18.37	17.50	17.31	16.8	16.37	2.945	2.875	quasar	3.005
094137.09+102650.9	2012 Apr 16	2700	18.67	18.04	17.90	17.9	17.75	17.01	16.77	16.38	15.84	2.535	2.625	quasar	2.584
095118.43+083959.9	2012 Mar 13	3600	18.90	18.25	18.21	18.19	18.02	17.50	17.18	16.64	15.85	2.365	2.375	quasar	2.523
100834.73−022302.5	2012 Apr 14	3600	19.93	18.13	17.91	17.88	17.85	17.39	16.95	16.54	16.01	3.005	2.975	quasar	3.086
103301.49+065106.5	2012 May 16	2700	18.73	18.03	17.91	17.84	17.69	17.15	16.88	16.45	16.05	2.565	2.625	quasar	2.637
114608.05+094216.5	2012 May 15	5400	19.54	18.49	18.49	18.38	17.96	17.05	16.83	16.22	15.35	2.615	2.475	quasar	2.580
115531.45−014611.9	2012 Mar 13	6000	23.25	19.36	18.91	18.50	18.50	17.94	17.39	17.00	16.36	3.495	3.350	quasar(BAL)	3.196
121510.62+142834.5	2012 Apr 15	3600	19.20	18.45	18.34	18.33	18.15	17.47	17.20	16.75	16.11	2.595	2.675	quasar	2.480
122043.86+011122.1	2012 May 17	3600	19.21	18.39	18.38	18.27	18.00	17.20	16.86	16.31	15.61	2.395	2.725	quasar	2.565
122619.73+104953.5	2012 Apr 15	3600	19.06	18.35	18.27	18.27	18.10	17.49	17.23	16.78	16.12	2.565	2.625	quasar	2.375
124605.36+071128.2	2012 Mar 14	3600	19.20	18.56	17.82	17.52	17.33	16.88	16.55	15.97	15.25	3.435	3.550	quasar	2.044
125934.29+075200.7	2012 May 16	2700	18.29	17.78	17.67	17.68	17.63	17.2	16.93	16.45	15.93	2.475	2.625	quasar	2.370
130318.32+030809.4	2012 Apr 14	2700	18.39	17.65	17.58	17.47	17.35	16.6	16.25	15.87	15.37	2.595	2.675	quasar	2.664
131008.67+084405.0	2012 Apr 16	2700	18.48	17.85	17.73	17.72	17.63	17.15	16.92	16.43	15.85	2.535	2.625	quasar	2.232
135942.50+022426.0	2012 Mar 14	3600	24.10	18.82	18.33	18.29	18.18	17.69	17.26	16.85	16.33	3.475	3.350	quasar(BAL)	3.265
142405.57+044105.5	2012 May 16	3600	18.72	18.17	18.01	18.01	17.83	17.36	17.09	16.50	15.89	2.465	2.625	quasar(BAL)	2.232
142543.33+024759.8	2012 Apr 15	2700	18.48	17.79	17.77	17.75	17.67	16.94	16.65	16.16	15.70	2.605	2.675	quasar	2.689
142854.09+132259.0	2012 May 17	5400	20.89	19.46	18.94	18.37	18.10	17.26	16.86	16.38	15.83	2.735	2.925	quasar	3.093
144526.15+023906.8	2012 May 15	3600	19.05	18.00	18.00	17.95	17.78	17.24	16.91	16.46	15.98	2.695	2.675	quasar	2.706
145230.38+130227.3	2012 May 17	2700	18.26	17.77	17.65	17.68	17.51	16.81	16.58	16.03	15.33	2.465	2.525	quasar	2.468
151321.18+012502.2	2012 Apr 16	3600	19.45	18.18	18.28	18.17	18.05	17.34	17.01	16.36	15.81	2.865	2.825	quasar	2.753
152808.87+005211.8	2012 Apr 16	3600	18.97	18.11	18.09	18.07	17.95	17.20	16.89	16.54	16.12	2.675	2.675	quasar	2.610
153303.54+064032.9	2012 Apr 15	3600	22.74	18.99	18.43	18.35	18.26	17.84	17.26	16.81	16.15	3.405	3.350	quasar	3.422
153319.44+043257.3	2012 Apr 14	5400	18.81	18.10	17.99	17.96	17.74	17.28	17.08	16.74	15.95	2.535	2.575	low S/N	
153515.55+291038.5	2012 Apr 14	2700	19.08	17.71	17.50	17.36	17.30	16.79	17.29	16.17	16.10	2.905	2.775	F star	
153550.13+063352.8	2012 May 17	3600	19.08	18.43	18.32	18.32	18.12	17.90	17.57	17.15	16.37	2.535	2.275	low S/N	
153551.88+044416.4	2012 May 16	3600	18.73	18.19	18.03	18.01	17.92	17.79	17.50	17.02	16.13	2.535	2.275	quasar	2.377
153951.05+020133.8	2012 May 16	3600	18.90	18.31	18.24	18.21	18.08	17.32	17.11	16.78	16.13	2.365	2.575	quasar	2.569
154503.23+015614.7	2012 May 16	2700	18.36	17.90	17.64	17.65	17.51	17.03	16.71	16.21	15.42	2.505	2.225	low S/N	
162352.69+230119.6	2012 May 15	5400	20.15	19.21	18.79	18.45	17.96	17.20	16.57	16.08	15.76	2.715	2.925	low S/N	
162620.89+282924.7	2012 Apr 15	3600	19.20	18.42	18.32	18.33	18.17	17.39	17.04	16.81	16.30	2.605	2.675	quasar	2.534

Notes. The SDSS *ugriz* magnitudes are given in the AB system and the UKIDSS *YJHK* magnitudes are given in the Vega system. z_{ph1}, z_{ph2}, and z_{sp} are the photometric redshifts obtained from the five-band SDSS data from Richards et al. (2009), the nine-band SDSS-UKIDSS data by us, and the spectral redshifts from our observations, respectively.

unidentified. This high success rate is largely due to the quasar candidate selection procedures we adopted, particularly the $Y - K/g - z$ criterion and the nine-band SDSS-UKIDSS photometric redshifts used to select $2.2 < z < 3.5$ quasar candidates. As we stated before, using photometric redshifts greater than 2.2 and redshift probabilities higher than 0.5 from R09 enables us to reduce the number of quasar candidates brighter than $i = 18.5$ from 8845 to 2149. In addition, using the $Y - K/g - z$ criterion, we can reduce the number of quasar candidates with SDSS-UKIDSS data from 401 to 126. Therefore, our high success rate in identifying $2.2 < z < 3.5$ quasars is not a surprise because we can efficiently exclude stellar contaminants by using the $Y - K/g - z$ criterion and we can select the most reliable $2.2 < z < 3.5$ quasar candidates using the photometric redshifts obtained from the SDSS or SDSS-UKIDSS photometric data.

3. THE ACCURACY OF PHOTOMETRIC REDSHIFTS AND STELLAR CONTAMINANTS IN THE QUASAR CANDIDATE CATALOG OF SDSS DR6

We selected the quasar targets from the SDSS DR6 1 million quasar candidate catalog of R09 and used both the SDSS and UKIDSS photometric data for further selection and photometric redshift estimates to achieve a high success rate in identifying $2.2 < z < 3.5$ quasars. With the SDSS-UKIDSS optical/near-IR data and our proposed quasar selection criterion,

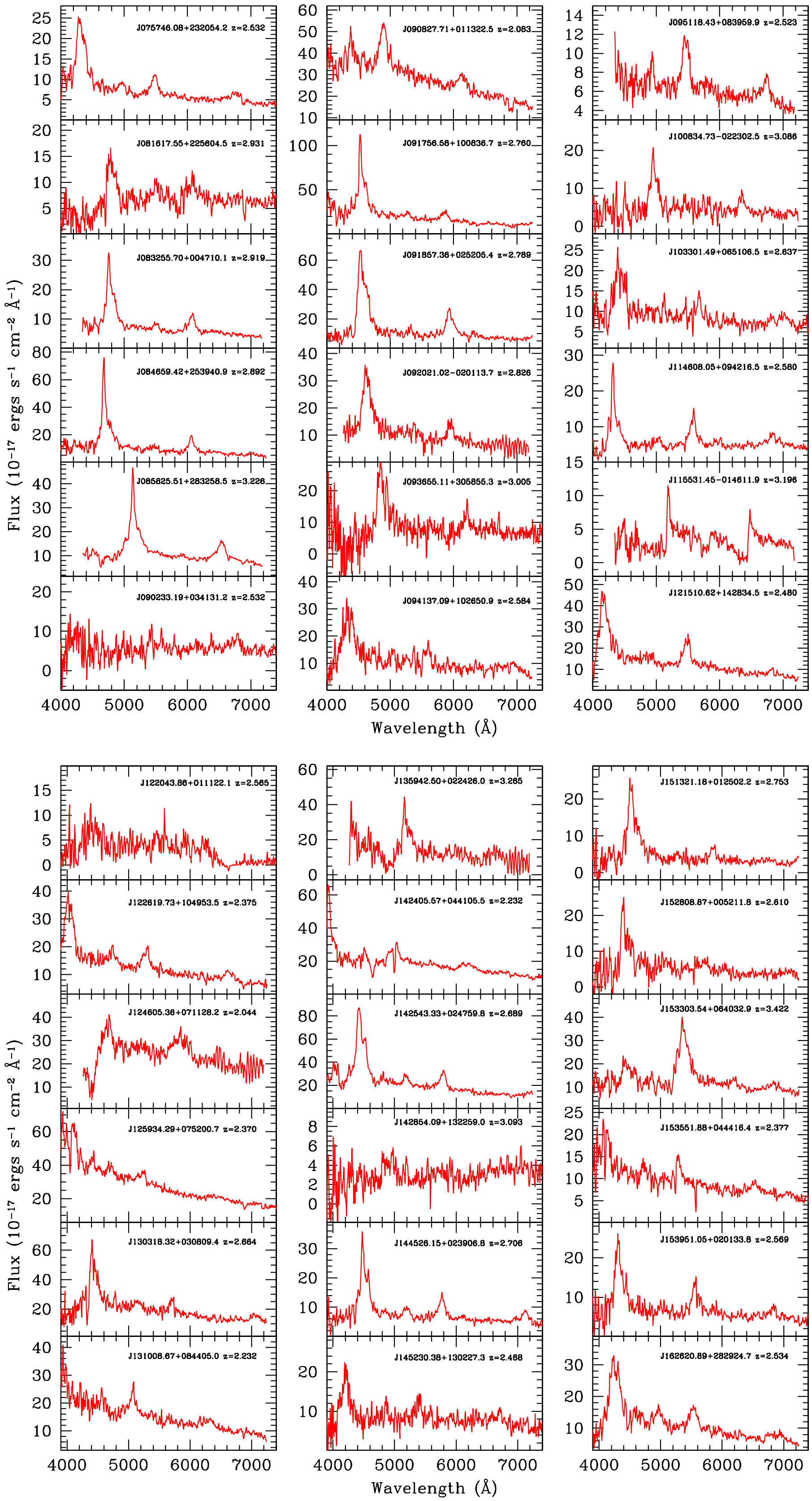

Figure 1. Spectra of the 36 new quasars at $2.2 < z < 3.5$ identified with the BFOSC of the Xinglong 2.16 m telescope, NAOC. The strongest emission line in each spectrum is Lyα+N V.

(A color version of this figure is available in the online journal.)

Table 3
Spectral Parameters and Black Hole Masses of 36 New Quasars

Name (SDSS J)	Redshift	Slope[a]	$\log(L_{1350})$ (erg s^{-1})	FWHM(C IV) (km s^{-1})	$\log(M_{BH})$ ($M_\odot$)	$\log(L_{bol})$ (erg s^{-1})	$\log(R_{EDD})$
J075746.08+232054.2	2.532 ± 0.007	−1.59	46.39	6000	9.48	47.06	−0.53
081617.55+225604.5	2.931 ± 0.007	−0.23	46.45	11538[b]	10.08	47.11	−1.07
083255.70+004710.1	2.919 ± 0.007	−0.95	46.43	4778	9.31	47.10	−0.31
084659.42+253940.9	2.892 ± 0.029	−1.80	46.54	4073	9.22	47.20	−0.12
085825.51+283258.5	3.226 ± 0.008	−1.32	46.74	6038	9.68	47.41	−0.37
090233.19+034131.2	2.532 ± 0.028	−0.39	46.30	7817[b]	9.66	46.96	−0.80
090827.71+011322.5	2.083 ± 0.081	−1.58	46.82	8314	9.99	47.48	−0.61
091756.58+100836.7	2.760 ± 0.026	−2.44	46.86	6797	9.84	47.52	−0.42
091857.36+025205.4	2.789 ± 0.038	−0.71	46.52	6306	9.59	47.18	−0.51
092021.02−020113.7	2.826 ± 0.025	−3.27	46.61	6278	9.64	47.27	−0.47
093655.11+305855.3	3.005 ± 0.012	0.01	46.44	4699	9.30	47.10	−0.29
094137.09+102650.9	2.584 ± 0.024	−0.99	46.54	4779[b]	9.36	47.20	−0.26
095118.43+083959.9	2.523 ± 0.006	−0.82	46.27	6448	9.48	46.94	−0.65
100834.73−022302.5	3.086 ± 0.012	−2.04	46.39	5209	9.36	47.05	−0.41
103301.49+065106.5	2.637 ± 0.027	−1.60	46.46	6817[b]	9.63	47.13	−0.61
114608.05+094216.5	2.580 ± 0.020	−0.90	46.11	6631	9.42	46.77	−0.75
115531.45−014611.9	3.196 ± 0.047	−1.87	46.29	8483[b]	9.73	46.96	−0.88
121510.62+142834.5	2.480 ± 0.073	−2.20	46.62	7208	9.76	47.29	−0.58
122043.86+011122.1	2.565 ± 0.042	1.00	45.95	3379[b]	8.75	46.62	−0.24
122619.73+104953.5	2.375 ± 0.046	−2.06	46.54	7050	9.70	47.20	−0.60
124605.36+071128.2	2.044 ± 0.019	−0.10	46.53	10662[b]	10.06	47.19	−0.96
125934.29+075200.7	2.370 ± 0.030	−2.02	46.91	11521[b]	10.33	47.57	−0.85
130318.32+030809.4	2.664 ± 0.037	−1.91	46.84	5772	9.69	47.50	−0.29
131008.67+084405.0	2.232 ± 0.050	−1.57	46.55	7262	9.73	47.21	−0.62
135942.50+022426.0	3.265 ± 0.014	−0.42	46.77	8215[b]	9.96	47.44	−0.62
142405.57+044105.5	2.232 ± 0.050	−1.05	46.56	11934[b]	10.17	47.22	−1.05
142543.33+024759.8	2.689 ± 0.035	−2.51	46.88	5984	9.74	47.55	−0.30
142854.09+132259.0	3.093 ± 0.015	0.02	46.10	5404[b]	9.24	46.77	−0.57
144526.15+023906.8	2.706 ± 0.017	−1.31	46.37	6040	9.48	47.03	−0.55
145230.38+130227.3	2.468 ± 0.015	−0.79	46.31	7693	9.66	46.98	−0.78
151321.18+012502.2	2.753 ± 0.035	−1.31	46.10	7759[b]	9.55	46.77	−0.89
152808.87+005211.8	2.610 ± 0.014	−0.77	46.17	12187[b]	9.98	46.83	−1.25
153303.54+064032.9	3.422 ± 0.021	−3.41	46.89	12183	10.36	47.56	−0.91
153551.88+044416.4	2.377 ± 0.025	−1.43	46.35	9027[b]	9.82	47.01	−0.90
153951.05+020133.8	2.569 ± 0.028	−1.88	46.29	8925	9.78	46.96	−0.92
162620.89+282924.7	2.534 ± 0.034	−0.85	46.48	7456	9.72	47.15	−0.67

Notes.
[a] The slope of the fitted power-law continuum.
[b] Only one Gaussian is fit to the entire C IV line profile.

we can also investigate the accuracy of photometric redshifts and the possible stellar contaminants in the SDSS DR6 quasar candidate catalog (R09), which will be helpful for future spectroscopic observations.

We cross-matched the SDSS DR6 1 million quasar candidate catalog of R09 with the UKIDSS/LAS DR8 data using a positional offset of 3″ for finding only the closest counterpart. We obtained 97,923 sources with full detections in the nine-band SDSS-UKIDSS data. This SDSS-UKIDSS quasar candidate sample is much larger than the previous one with 42,133 sources from the UKIDSS/LAS DR3 (Peth et al. 2011). Among these 97,923 sources, there are 24,878 known quasars and 73,011 unidentified quasar candidates in SDSS DR6.

First, we checked the improvement in the photometric redshift estimates using the nine-band SDSS-UKIDSS photometric data over the SDSS data alone. We used our photometric redshift estimation program (Wu & Jia 2010; Wu et al. 2004) to obtain the photometric redshifts of all unidentified quasar candidates and known quasars in R09 based on the SDSS-UKIDSS data and compared these redshifts with the photometric redshifts given in R09 and the spectral redshifts for known quasars in SDSS DR6. In the top two panels of Figure 2, we compare the photometric redshifts from R09 and our redshifts for 73,011 unidentified quasar candidates in R09 and show a histogram distribution of their differences. For 59.8% of these unidentified quasar candidates, the two kinds of photometric redshifts differ by less than 20%. However, there are still obvious differences, especially when the photometric redshifts are smaller than 3. Compared with our results, the photometric redshifts given in R09 are systematically larger for some low-redshift quasar candidates. In the two middle and lower panels of Figure 2, we compare the photometric redshifts given in R09 and those calculated by us for 24,878 known quasars with spectral redshifts, respectively (the two middle panels are similar to Figure 7 in Peth et al. (2011) but with more known quasars because we used the data in UKIDSS/LAS DR8). For 76.1% of the known quasars, R09 calculated photometric redshifts that differed from the spectral redshifts by less than 20%. By using the SDSS-UKIDSS nine-band photometric data to estimate the photometric redshifts, the fraction increases to 85.2%. This significant improvement can be clearly observed in Figure 2 and demonstrates again that by adding the near-IR photometric data

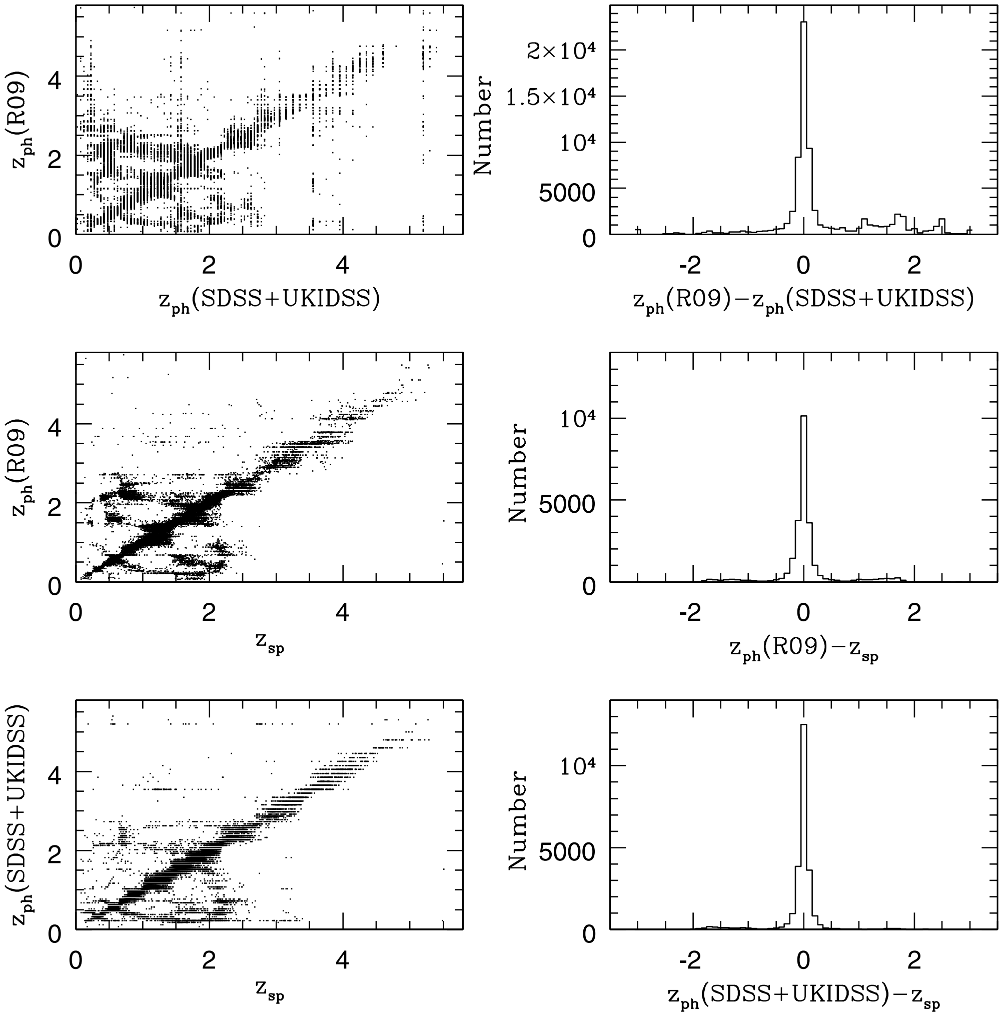

Figure 2. Top panels: comparison of the photometric redshifts from R09 and our redshifts based on SDSS-UKIDSS nine-band data for 73,011 unidentified quasar candidates in R09 and the histogram distribution of their differences. Middle panels: comparison of the photometric redshifts from R09 with the spectral redshifts for 24,878 known quasars and the histogram distribution of their differences. Bottom panels: comparison of the photometric redshifts calculated by us with the spectral redshifts for 24,878 known quasars and the histogram distribution of their differences.

to the SDSS optical data we can achieve a substantially higher accuracy in photometric redshift esimates (Wu & Jia 2010; Wu et al. 2012).

Next, we checked for possible stellar contaminants in the quasar candidate catalog of SDSS DR6 (R09), using the $Y - K/g - z$ quasar selection criterion. In Figure 3, we show the distributions of 24,878 known quasars and 73,011 unidentified quasar candidates in R09 in the $Y - K/g - z$ color–color diagram, as well as our $Y - K/g - z$ quasar selection criterion (Wu & Jia 2010). For 24,648 known $z < 4$ quasars, we can select 24,295 objects (98.6%) using the $Y - K/g - z$ criterion. For 61,489 unidentified quasar candidates in R09 with photometric redshifts $z_{ph} < 2.2$ (we adopted the photometric redshifts estimated with the SDSS-UKIDSS nine-band photometric data), we can select 60,412 objects (98.3%) using the $Y - K/g - z$ criterion. For 10,687 unidentified quasar candidates in R09 with photometric redshifts $2.2 < z_{ph} < 4$, we can select 8,934 objects (83.6%) using the $Y - K/g - z$ criterion. Therefore, the quasar candidate selection in R09 is fully consistent with our $Y - K/g - z$ selection for $z_{ph} < 2.2$ quasar candidates, but there are substantial stellar contaminants when selecting $2.2 < z_{ph} < 4$ quasar candidates. This fact can be also seen from the lower panel of Figure 3, where the green dots below the line most probably represent stellar contaminants.

To better understand the quasar selection efficiency and the stellar contaminants at different redshifts, we plot in Figure 4 the photometric redshift dependences of the fraction of 24,648 known $z < 4$ quasars selected by the $Y - K/g - z$ criterion and the fraction of 72,176 unidentified quasar candidates in R09 with photometric redshifts $z_{ph} < 4$ selected by the $Y - K/g - z$ criterion. For the known $z < 4$ quasars, using the $Y - K/g - z$ criterion can produce an efficiency higher than 90% at almost all redshifts, except for $z > 3.5$. For the unidentified quasar candidates, the R09 selection has a similar efficiency (higher than 90%) as using the $Y - K/g - z$ criterion for selecting $z_{ph} < 2.6$ quasars but has a higher rate of stellar contaminants when selecting $z_{ph} > 2.6$ quasars. One may think that the decrease of the quasar selection fraction at $z_{ph} > 2.6$ (denoted by the blue dotted line in Figure 4) is due to both the misidentification of quasars as stars by the $Y - K/g - z$ criterion and true stellar contaminants. After deducing the misidentification rate of quasars as stars by the $Y - K/g - z$ criterion at different redshifts (which can be estimated from the known quasar selection fraction denoted by the black solid line in Figure 4), we can obtain the possible stellar contamination rate in R09 at different redshifts (denoted by the red dashed line in Figure 4). It is clear that the stellar contamination rate becomes substantially higher for selecting

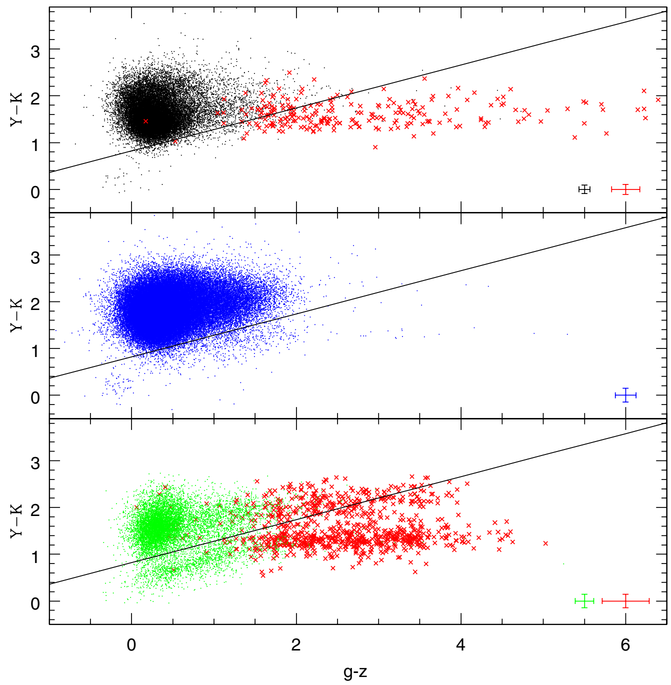

Figure 3. Top panel: the distribution of 24,878 known quasars in R09 in the $Y - K/g - z$ color–color diagram. Black dots represent $z < 4$ quasars and red crosses represent $z > 4$ quasars. Middle panel: the distribution of 61,489 unidentified quasar candidates in R09 with photometric redshifts $z_{ph} < 2.2$ in the $Y - K/g - z$ color–color diagram. Bottom panel: the distribution of 10,687 unidentified quasar candidates in R09 with photometric redshifts $2.2 < z_{ph} < 4$ (green dots) and 835 unidentified quasar candidates in R09 with photometric redshifts $z_{ph} > 4$ (red crosses) in the $Y - K/g - z$ color–color diagram. The error bars in the lower-right part of each panel denote the typical color uncertainty of quasars at different redshifts.

(A color version of this figure is available in the online journal.)

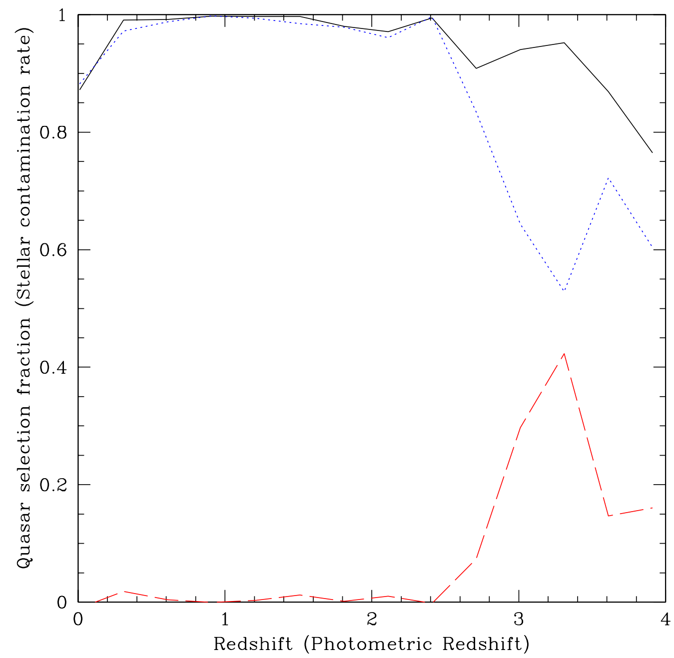

Figure 4. Black solid line denotes the redshift dependence of the fraction of 24,648 known $z < 4$ quasars in R09 selected with the $Y - K/g - z$ criterion. The blue dotted line denotes the fraction of 72,176 unidentified quasar candidates in R09 with photometric redshifts $z_{ph} < 4$ selected with the $Y - K/g - z$ criterion as a function of photometric redshift. The red dotted line denotes the possible stellar contamination rates of these unidentified quasar candidates in R09 at different photometric redshifts.

(A color version of this figure is available in the online journal.)

$z_{ph} > 2.6$ quasars than lower redshift quasars, even up to 30% to 40% for selecting quasars at redshifts $3 < z_{ph} < 3.5$. We must note that the real stellar contamination rate is probably much higher than what we estimated with the $Y - K/g - z$ criterion. Therefore, the stellar contamination rate in R09 that we obtained from selecting $2.6 < z_{ph} < 4$ quasars could be underestimated. In fact, based on the clustering study of Myers et al. (2006), the stellar contamination in the "mid-z" range of R09 was estimated to be higher than 50% (Richards et al. 2009). Nevertheless, we believe that using the $Y - K/g - z$ criterion can help us to significantly exclude stellar contamination and obtain a higher efficiency at selecting $2.6 < z_{ph} < 4$ quasars.

From R09, we can obtain a list of SDSS DR6 unidentified quasar candidates with UKIDSS/LAS DR8 full detections in the *YJHK* bands and with photometric redshifts $2.2 \leqslant z_{ph}(R09) \leqslant 3.5$. This sample consists of 17,719 objects. However, if we adopt our photometric redshifts obtained from the nine-band SDSS-UKIDSS photometric data and use our $Y - K/g - z$ criterion to do further selection, such a list consists of only 7727 quasar candidates at $2.2 \leqslant z_{ph} \leqslant 3.5$. The substantial decrease in sample size is mainly due to the increase in the photometric redshift reliability and the decrease in stellar contaminants resulting from using the $Y - K/g - z$ criterion. In Table 4, we list the name, photometric redshift, and SDSS and UKIDSS magnitudes for these 7727 quasar candidates with estimated photometric redshifts $2.2 \leqslant z_{ph} \leqslant 3.5$. We noticed that some of these objects have been identified after SDSS DR6, including this work. Future spectroscopy of these unidentified quasar candidates will provide further checks on the robustness of both the quasar selection criterion and the photometric redshift estimation method.

4. COMPARISONS WITH SDSS-III DR9 QUASARS

Very recently, SDSS-III/BOSS released the DR9 quasar catalog, which consists of 87,822 quasars (78,086 are new and 61,931 have redshifts higher than 2.15) detected over a sky area of 3275 deg^2 (Paris et al. 2012). This catalog provides us a chance to check the effectiveness of our proposed $Y - K/g - z$ criterion with the largest sample of $z > 2.1$ quasars currently available.

After cross-matching the SDSS-III DR9 quasar catalog with the UKIDSS/LAS DR8 catalog, 17,999 out of 87,822 quasars have available *Y* and *K*-band data, with a sampling rate of 20.5%. 17,308 of these 17,999 quasars satisfy the $Y - K/g - z$ selection criterion for $z < 4$ quasars, with a completeness rate of 96.2%. In the top panel of Figure 5, we show the distributions of 17,999 SDSS-III/DR9-UKIDSS/LAS/DR8 (hereafter DR9-UKIDSS) quasars in the $Y - K/g - z$ color–color diagram and compare these objects with objects meeting our proposed $Y - K/g - z$ selection criterion for $z < 4$ quasars. Similar to the upper panel of Figure 3, this comparison also clearly demonstrates the effectiveness of the $Y - K/g - z$ selection criterion in selecting $z < 4$ quasars.

We also check whether the $Y - K/g - z$ selection depends on magnitude and redshift. In the middle panel of Figure 5, we show the magnitude dependence of the selection fraction of 17,999 DR9-UKIDSS quasars on our $Y - K/g - z$ criterion and the normalized magnitude distributions (fraction of the number of quasars in each magnitude bin ratioed to total number) for 17,308 quasars selected with the $Y - K/g - z$ criterion and the 87,822 SDSS-III/DR9 quasars. The comparison shows that

Table 4
A Catalog of 7727 SDSS-UKIDSS Quasar Candidates at $2.2 \leqslant z_{ph} \leqslant 3.5$ Selected from R09

Name (SDSS J)	$z_{ph}(R09)$	z_{ph}	u	g	r	i	z	Y	J	H	K
000005.95+145310.1	2.255	2.725	21.31	20.64	20.45	20.19	19.93	19.41	18.83	18.51	17.76
000035.59−003146.1	2.255	2.725	21.63	21.04	20.83	20.4	20.36	19.19	18.92	18.31	17.51
000041.87−001207.3	2.905	2.925	21.02	19.62	19.44	19.32	19.19	18.45	18.14	17.56	16.86
000050.59+010959.1	2.605	2.575	19.85	19.08	19.02	19.09	18.89	18.33	18.17	17.69	16.9
000201.15+001707.4	2.465	2.475	21.48	20.77	20.69	20.65	20.18	19.71	19.36	18.77	17.68

Notes. The SDSS *ugriz* magnitudes are given in the AB system and the UKIDSS *YJHK* magnitudes are given in the Vega system. $z_{ph}(R09)$ and z_{ph} are the photometric redshifts obtained from the five-band SDSS data from Richards et al. (2009) and the nine-band SDSS-UKIDSS data by us, respectively.

(This table is available in its entirety in machine-readable and Virtual Observatory (VO) forms in the online journal. A portion is shown here for guidance regarding its form and content.)

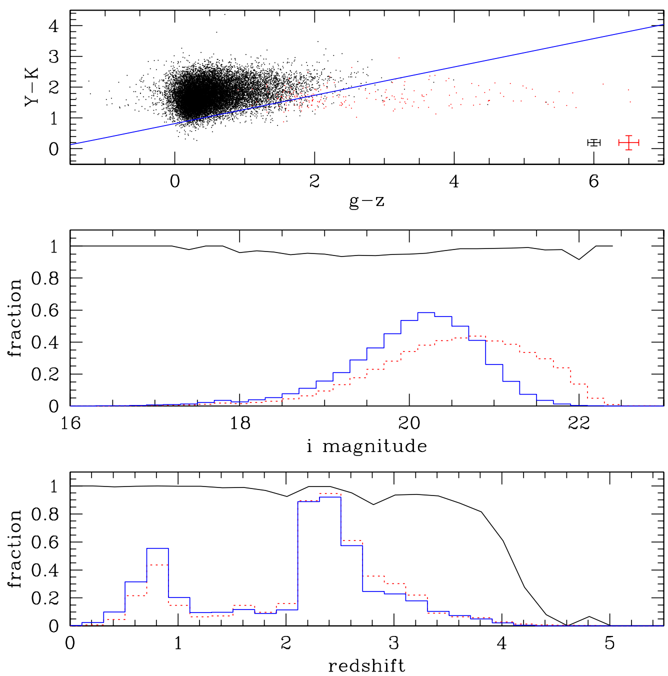

Figure 5. Top panel: the distributions of 17,999 SDSS-III/DR9-UKIDSS/LAS/DR8 quasars in the $Y - K/g - z$ color–color diagram. Quasars with redshifts smaller (higher) than 4 are denoted as black (red) points. The black (red) error bars in the lower right corner denote the typical color uncertainty of quasars with redshifts smaller (higher) than 4. The blue solid line represents our proposed $Y - K/g - z$ selection criterion for $z < 4$ quasars. Middle panel: the black solid line represents the magnitude dependence of the selection fraction of 17,999 DR9-UKIDSS quasars on our $Y - K/g - z$ criterion. The blue and red histograms show the normalized magnitude distributions (fraction of the number of quasars in each magnitude bin ratioed to the total number) of 17,308 quasars selected with the $Y - K/g - z$ criterion and 87,822 SDSS-III/DR9 quasars, respectively. Bottom panel: the black solid line represents the redshift dependence of the selection fraction of 17,999 DR9-UKIDSS quasars by our $Y - K/g - z$ criterion. The blue and red histograms show the normalized redshift distributions (fraction of the number of quasars in each redshift bin ratioed to the total number) of 17,308 quasars selected by the $Y - K/g - z$ criterion and 87,822 SDSS-III/DR9 quasars, respectively. For clarity, all histograms in the middle and bottom panels are magnified by a factor of five.

(A color version of this figure is available in the online journal.)

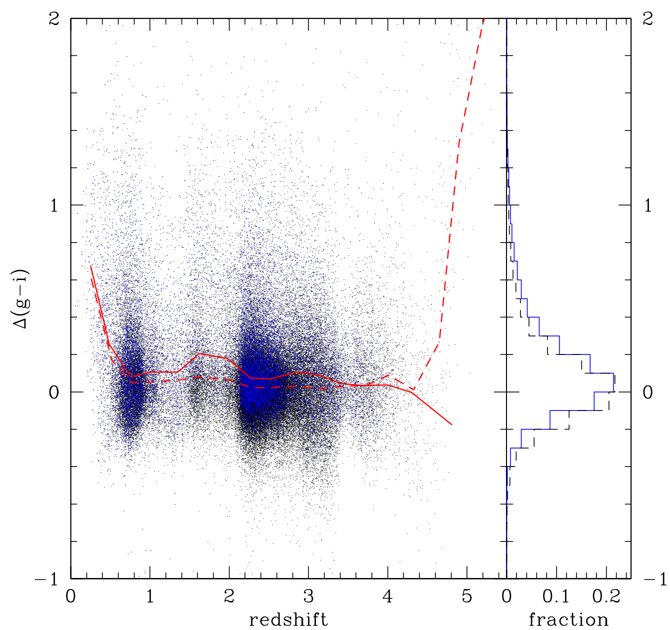

Figure 6. Distributions of $\Delta(g - i)$ vs. redshift for 17,308 quasars selected with the $Y - K/g - z$ criterion (blue points) and 87,822 SDSS-III/DR9 quasars (black points). The red solid and dashed lines show the distributions of median $\Delta(g - i)$ values in each redshift bin for these two quasar samples. The blue solid and black dashed histograms shows the distributions of normalized $\Delta(g - i)$ values (fraction of the number of quasars in each $\Delta(g - i)$ bin ratioed to the total number of quasars) over the whole redshift range of these two samples. The quasar sample selected with the $Y - K/g - z$ criterion is slightly redder than the SDSS-III/DR9 quasar sample at $z < 4$.

(A color version of this figure is available in the online journal.)

by using UKIDSS data we do select optically brighter quasars (especially those brighter than $i = 20.5$) due to the limited sensitivity of UKIDSS. However, the selection efficiency of using the $Y - K/g - z$ criterion does not significantly depend on magnitude for quasars with UKIDSS data at $i < 20.5$. In the bottom panel of Figure 5, we show the redshift dependence of the selection fraction of the 17,999 DR9-UKIDSS quasars obtained with our $Y - K/g - z$ criterion; this panel clearly shows that our criterion is robust for selecting $z < 4$ quasars. Comparing the normalized redshift distributions (fraction of the number of quasars in each redshift bin ratioed to the total number) of the 17,308 quasars selected with the $Y - K/g - z$ criterion and the 87,822 SDSS-III/DR9 quasars also demonstrates the similarities in the distributions of these two populations.

In addition, we need to check whether using the $Y - K/g - z$ criterion results in quasars with specific colors. In Figure 6, we show the distribution of $\Delta(g - i)$ versus redshift for the 17,308 quasars selected with the $Y - K/g - z$ criterion and the 87,822 SDSS-III/DR9 quasars. Obviously, these populations significantly overlap at $z < 4$. From the distribution of median $\Delta(g - i)$ values in each redshift bin, the quasars selected with the $Y - K/g - z$ criterion have slightly redder $g - i$ colors than the SDSS-III/DR9 quasars at $z < 4$. The median $\Delta(g - i)$ value for the 17,308 quasars selected with the $Y - K/g - z$ criterion is 0.088, which is slightly redder that the median value of 0.035 for the 87,822 SDSS-III/DR9 quasars. This result occurs mainly because we mostly select quasars with $i < 20.5$ using the UKIDSS near-IR data (see the middle panel of Figure 5). Most SDSS-III/DR9 quasars with $i > 20.5$ have smaller or negative $\Delta(g-i)$ values. We also noticed that the SDSS-III/DR9 quasars with $i < 20.5$ have a median $\Delta(g-i)$ value of 0.080, which is close to the median value of 0.088 of the $Y - K/g - z$ selected quasars.

Finally, we check whether using the $Y - K/g - z$ criterion can help us to select more BAL quasars. In SDSS-III/DR9 quasar catalog, 7,533 quasars are found to be BAL quasars after visual inspection. 2,173 of these objects have UKIDSS/LAS DR8 data and 1,974 quasars satisfy the $Y - K/g - z$ criterion (90.8%). This fraction is only slightly smaller than the 96.2% rate obtained for the $Y - K/g - z$ selection of all DR9-UKIDSS quasars, implying that we can also efficiently select BAL quasars using the $Y - K/g - z$ criterion. We also noticed that three quasars in our 36 newly discovered quasars are BAL quasars (see Section 2), which is consistent with the fraction of 7,533 BAL quasars in 87,822 SDSS-III/DR9 quasars, although we acknowledge small number statistics.

5. SELECTING RED QUASARS AND TYPE II QUASARS WITH THE $Y - K/g - z$ CRITERION

In this section, we check whether we can also efficiently select red quasars and type II quasars using the $Y - K/g - z$ criterion.

Glikman et al. (2007, 2012) presented a sample of 128 red quasars at $z < 3.05$, selected from the FIRST-2MASS radio and near-IR surveys. These quasars with red colors, $J{-}K > 1.7$, are thought to be objects transitioning between heavily obscured quasars and normal blue quasars. Urrutia et al. (2009) also identified 57 red quasars with $J{-}K > 1.3$ from 122 candidates selected from FIRST, 2MASS, and SDSS, with a high fraction of BAL quasars. By cross-matching with the UKIDSS LAS/DR8 catalog, we obtain 26 and 16 red quasars with Y and K-band detections from these two samples, respectively. We plot these objects in the $Y - K/g - z$ color–color diagram (see the upper panel of Figure 7) and find that 23 out of 26 red quasars and 14 out of 16 red quasars in these two samples satisfy the $Y - K/g - z$ criterion. The selection efficiency is 88.5% and 87.5% for these two samples, respectively. This comparison clearly demonstrates the high efficiency of selecting red quasars with the $Y - K/g - z$ criterion.

Because the SDSS-III/DR9 quasar catalog does not provide information about how many type II quasars are included, we use the existing type II quasar catalog in SDSS to check the efficiency of selecting type II quasars with the $Y - K/g - z$ criterion. Using the catalog provided by Reyes et al. (2010), which includes 887 optically selected $0.3 < z < 0.83$ type II SDSS quasars, we find that 282 out of 887 type II quasars have available Y and K-band data from UKIDSS LAS/DR8. We plot these objects in the $Y - K/g - z$ color–color diagram and overplot the $Y - K/g - z$ selection criterion (see the lower panel of Figure 7). 272 of these 282 type II quasars (96.5%) satisfy our $Y - K/g - z$ criterion. This selection fraction is similar to the 96.2% fraction for the $Y - K/g - z$ selection of all DR9-UKIDSS quasars, which indicates that we can also efficiently discover type II quasars using the $Y - K/g - z$ criterion.

In Figure 7, we also plot the predicted color tracks for type I and type II quasars at different redshifts using the related spectral templates from Polletta et al. (2007). We can clearly see that

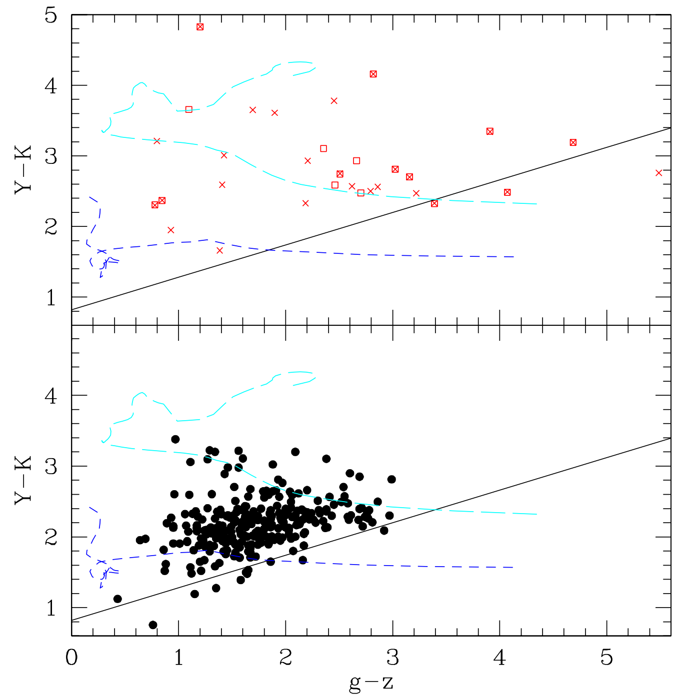

Figure 7. Top panel: red quasars with UKIDSS data in the $Y - K/g - z$ diagram. Red crosses and squares denote red quasars from Glikman et al. (2012) and Urrutia et al. (2009), respectively. There are 11 quasars in common between these two samples. Bottom panel: optically selected type II quasars with UKIDSS data in the $Y - K/g - z$ diagram. Filled circles denote type II quasars from Reyes et al. (2010). In both panels, black lines denote the $Y - K/g - z$ selection criterion. Blue and cyan dashed lines represent the predicted colors of type I and type II quasars, respectively, at different redshifts (up to $z = 4.3$ near the right end of the dashed lines) using the templates from Polletta et al. (2007).

(A color version of this figure is available in the online journal.)

although type II quasars have redder $Y{-}K$ and $g{-}z$ colors than type I quasars, we can efficiently select both type I and type II quasars at redshifts up to 4 using the $Y - K/g - z$ criterion.

6. CAN WE USE THE $Y - K/g - z$ CRITERION TO SELECT MORE $2.2 < z < 3.5$ QUASARS?

Although our above test with the recently released SDSS-III/DR9 quasar catalog does indicate the effectiveness of using the $Y - K/g - z$ criterion in selecting $z < 4$ quasars, one question still needs to be addressed. Can we use the $Y - K/g - z$ criterion to select additional $2.2 < z < 3.5$ quasars that SDSS-III/BOSS does not select?

To answer this question, we need to find a sky area that is covered both by SDSS-III/BOSS and UKIDSS. We also need to compare the quasar candidates selected by the SDSS-III/BOSS and $Y - K/g - z$ selection criteria. We utilized a photometric catalog of a 15 deg^2 region in SDSS Stripe 82 (with $36^\circ <$ R.A. $< 42^\circ$ and $-1^\circ\!.25 <$ Decl. $< 1^\circ\!.25$), which has relatively complete spectroscopic observations of SDSS-III/BOSS quasar targets. By cross-matching the 90,922 SDSS sources in this area with UKIDSS and selecting sources with SDSS photometric parameters type = 6, $r < 21.85$, and $g < 22$ (as in SDSS-III/BOSS, r and g magnitudes are Galactic extinction-corrected), we obtain 24,627 point sources with UKIDSS/LAS Y and K-band detections. Among these point sources, 21,715 were unidentified while 2,912 were identified (including 743 quasars and 2,169 stars). 135 out of 743 identified quasars are in a redshift range between 2.2 and 3.5. 130 of them were included in the SDSS-III/DR9 quasar catalog and five of them were identified by other BOSS ancillary programs. We also found that 712 out of 743 identified quasars, including 126 out of 135 $2.2 < z < 3.5$ quasars, satisfy the $Y - K/g - z$ selection criterion.

Among 21,715 unidentified sources, 340 satisfy the $Y - K/g - z$ selection criterion. The photometric redshifts of these 340 quasar candidates were estimated based on their SDSS and UKIDSS data and 140 sources were found to have photometric redshifts between 2.2 and 3.5. If we further require the χ^2 values of their photometric redshift estimations (Wu & Jia 2010; Wu et al. 2004; Weinstein et al. 2004) to be smaller than 10, which is satisfied by 94% of 743 identified quasars in this sky area, the number of $2.2 < z < 3.5$ quasar candidates selected by the $Y - K/g - z$ criterion becomes 86. Even if we require χ^2 values smaller than six, which is satisfied by 80% of the 743 known quasars in this area, the number of $Y - K/g - z$ selected $2.2 < z < 3.5$ quasar candidates becomes 52. Because there are 470 known $2.2 < z < 3.5$ quasars (421 are SDSS-III/DR9 quasars) in this sky area and 135 of them (mostly the brighter ones) have UKIDSS Y and K-band detections, the $Y - K/g - z$ selected additional $2.2 < z < 3.5$ quasar candidates may add at least 10% to the total number of SDSS-III/BOSS $2.2 < z < 3.5$ quasars. However, whether these candidates are real $2.2 < z < 3.5$ quasars still needs to be confirmed by future spectroscopic observations. Therefore, with this check we believe that SDSS-III/BOSS has selected most $2.2 < z < 3.5$ quasars and the $Y - K/g - z$ selection may add about 10% more $2.2 < z < 3.5$ quasars in the UKIDSS surveyed area.

7. DISCUSSION

We have presented spectroscopic observations of 43 bright quasar candidates selected from R09, which have photometric redshifts $2.2 < z_{ph} < 3.5$ estimated from the nine-band SDSS and UKIDSS photometric data and satisfy our $Y - K/g - z$ criterion. We have successfully identified 36 of these objects to be real quasars with redshifts between 2.1 and 3.4. The high efficiency of the spectroscopic identifications provides further support for discovering more quasars at intermediate redshifts based on optical and near-IR color selections. We also found substantial improvement in the photometric redshift estimates when we used nine-band SDSS-UKIDSS data rather than SDSS data alone. We investigated the stellar contamination rate of quasar candidates in R09, which could be much higher for selecting quasars at photometric redshifts $3 < z_{ph} < 3.5$ than lower redshift quasars ($z < 2.2$). By using our photometric redshifts estimated from the SDSS and UKIDSS photometric data and the $Y - K/g - z$ criterion to exclude stellar contaminants, we obtained a catalog of 7727 SDSS-UKIDSS unidentified quasar candidates with photometric redshifts $2.2 < z_{ph} < 3.5$. Ongoing and future spectroscopic observations such as SDSS-III/BOSS(Eisenstein et al. 2011) will provide a further check on the robustness of this catalog, although the UKIDSS near-IR data were not used for selecting the majority of the quasar candidates in BOSS (Ross et al. 2012).

Using the recently released SDSS-III/DR9 quasar catalog and UKIDSS/LAS DR8 data, we find that 96.2% of UKIDSS-detected DR9 quasars, including 90.8% of BAL quasars, satisfy the $Y - K/g - z$ criterion. This result provides further support for using this criterion for selecting $z < 4$ quasars, including BAL quasars. We also check the efficiency of using the $Y - K/g - z$ criterion to select red quasars and type II quasars with some available samples and find that about 88% of red quasars at $z < 3.05$ and 96.5% of type II quasars at $z < 0.83$ satisfy the $Y - K/g - z$ criterion. These results, together with the predicted color tracks from different spectral templates of quasars, support the robustness of using the $Y - K/g - z$ criterion to discover both unobscured and obscured quasars. Our test in a small sky area of SDSS Stripe 82 also proves that with the $Y - K/g - z$ selection criterion we may add about 10% more $2.2 < z < 3.5$ quasars to the SDSS-III/BOSS quasars in the UKIDSS surveyed area.

Since UKIDSS only covers a very limited sky area, we still need much deeper optical/near-IR photometry in a larger sky area for taking full advantage of optical/near-IR color selection, especially for $z > 2.2$ quasars. The recently released Wide-field Infrared Survey Explorer all-sky data (Wright et al. 2010) also provided abundant photometric data in the near(middle)-IR bands, which will be very helpful for quasar selection (Wu et al. 2012; Stern et al. 2012; Edelson & Malkan 2012; Yan et al. 2013). Fortunately, several ongoing optical and near-IR photometric sky surveys will also provide us further opportunities to apply our optical/near-IR color selection of quasars to larger and deeper fields. In addition to SDSS III (Eisenstein et al. 2011), which has taken additional imaging over 2,500 deg^2 in the south Galactic cap, the SkyMapper (Keller et al. 2007) and Dark Energy Survey (The Dark Energy Survey Collaboration 2005) will also present multi-band optical photometry in 20,000/5,000 deg^2 of the southern sky, with a magnitude limit of 22/24 mag in the i-band, respectively. The Visible and Infrared Survey Telescope for Astronomy (VISTA; Arnaboldi et al. 2007) is carrying out the VISTA Hemisphere Survey in the near-IR $YJHK$ bands for 20,000 deg^2 of the southern sky with a magnitude limit of $K = 20.0$, which is about five and two magnitudes deeper than 2MASS (Skrutskie et al. 2006) and UKIDSS/LAS limits (Lawrence et al. 2007), respectively. Therefore, the optical and near-IR photometric data obtained with these ongoing surveys will provide us a large database for quasar selections. Needless to say, the ongoing Panoramic Survey Telescope & Rapid Response System (Kaiser et al. 2002) and the future Large Synoptic Survey Telescope (Ivezic et al. 2008) will also provide us with multi-epoch photometry in multiple bands covering a large area of the sky, which will undoubtedly help us to construct a much larger sample of quasars based on both optical/near-IR colors and variability features.

On the other hand, spectroscopic observations are still crucial to determining the quasar nature and redshifts of the quasar candidates selected from the optical/near-IR colors. The ongoing SDSS-III/BOSS is expected to obtain spectra of 150,000 quasars at $2.2 < z < 4$ (Eisenstein et al. 2011; Ross et al. 2012). We believe that many $2.2 < z < 3.0$ quasars, including the candidates we listed in this paper, should be spectroscopically identified by BOSS. In addition, the Chinese GuoShouJing telescope (Su et al. 1998; Cui et al. 2012; Zhao et al. 2012), a spectroscopic telescope with 4000 fibers that has finished the commissioning phase and started regular spectroscopic surveying in the fall of 2012, is also aimed at discovering 150,000 quasars from 0.5 million candidates with magnitudes brighter than $i = 20.2$ in the next five years (Wu et al. 2010a, 2010b; Wu 2011). By using optical/near-IR colors, we hope that larger input catalogs of reliable quasar candidates will be made available to these quasar surveys for future spectroscopic observations. We expect that a much larger and more complete quasar sample covering a wider range of redshifts will be constructed in the near future. In addition, the results we presented in this work may be also helpful for future spectroscopic surveys of quasars such as eBOSS and Big BOSS (Schlegel et al. 2011).

We thank the referee, Nicholas Ross, for very constructive suggestions that improved the paper. We also thank Adam Myers in the SDSS-III/BOSS team for providing us a photometric catalog of an eBOSS test region in SDSS Stripe 82. This work was supported by the National Natural Science Foundation of China (grant No. 11033001) and by the Open Project Program of the Key Laboratory of Optical Astronomy, NAOC, CAS.

Funding for the SDSS and SDSS-II has been provided by the Alfred P. Sloan Foundation, the Participating Institutions, the National Science Foundation, the US Department of Energy, the National Aeronautics and Space Administration, the Japanese Monbukagakusho, the Max Planck Society, and the Higher Education Funding Council for England. The SDSS Web site is http://www.sdss.org/.

The SDSS is managed by the Astrophysical Research Consortium for the Participating Institutions. The Participating Institutions are the American Museum of Natural History, Astrophysical Institute Potsdam, University of Basel, University of Cambridge, Case Western Reserve University, University of Chicago, Drexel University, Fermilab, the Institute for Advanced Study, the Japan Participation Group, Johns Hopkins University, the Joint Institute for Nuclear Astrophysics, the Kavli Institute for Particle Astrophysics and Cosmology, the Korean Scientist Group, the Chinese Academy of Sciences (LAMOST), Los Alamos National Laboratory, the Max-Planck-Institute for Astronomy (MPIA), the Max-Planck-Institute for Astrophysics (MPA), New Mexico State University, Ohio State University, University of Pittsburgh, University of Portsmouth, Princeton University, the United States Naval Observatory, and the University of Washington.

Facilities: Sloan (SDSS), UKIRT, Beijing:2.16m

REFERENCES

Arnaboldi, M., Neeser, M. J., Parker, L. C., et al. 2007, Msngr, 127, 28
Becker, R. H., White, R. L., & Helfand, D. J. 1995, ApJ, 450, 559
Boroson, T. A., & Green, R. F. 1992, ApJS, 80, 109
Boyle, B. J., Shanks, T., Croom, S. M., et al. 2000, MNRAS, 317, 1014
Butler, N. R., & Bloom, J. S. 2011, AJ, 141, 93
Casali, M., Adamson, A., Alves de Oliveira, C., et al. 2007, A&A, 467, 777
Chiu, K., Richards, G. T., Hewett, P. C., & Maddox, N. 2007, MNRAS, 375, 1180
Cristiani, S., Trentini, S., La Franca, F., et al. 1996, A&A, 306, 395
Croom, S. M., Smith, R. J., Boyle, B. J., et al. 2004, MNRAS, 349, 1397
Croom, S. M., Warren, S. J., & Glazebrook, K. 2001, MNRAS, 328, 150
Cui, X.-Q., Zhao, Y.-H., Chu, Y.-Q., et al. 2012, RAA, 12, 1197
Edelson, R., & Malkan, M. A. 2012, ApJ, 751, 52
Eisenstein, D., Weinberg, D. H., Agol, E., et al. 2011, AJ, 142, 72
Fan, X. 1999, AJ, 117, 2528
Fan, X., Narayanan, V. K., Lupton, R. H., et al. 2001a, AJ, 122, 2833
Fan, X., Strauss, M. A., Schneider, D. P., et al. 2001b, AJ, 121, 54
Gibson, R. R., Jiang, L., Brandt, W. N., et al. 2009, ApJ, 692, 758
Giveon, U., Maoz, D., Kaspi, S., Netzer, H., & Smith, P. S. 1999, MNRAS, 306, 637
Glikman, E., Helfand, D. J., White, R. L., et al. 2007, ApJ, 667, 673
Glikman, E., Urrutia, T., Lacy, M., et al. 2012, ApJ, 757, 51
Green, P. J., Schartel, N., Anderson, S. F., et al. 1995, ApJ, 450, 51
Greenstein, J. L., & Matthews, T. 1963, Natur, 197, 1041
Hambly, N., Collins, R. S., Cross, N. J. G., et al. 2008, MNRAS, 384, 637
Hazard, C., Mackey, M. B., & Shimmins, A. J. 1963, Natur, 197, 1037
Hennawi, J. F., Myers, A. D., Shen, Y., et al. 2010, ApJ, 719, 1672
Hewett, P. C., Warren, S. J., Leggett, S. K., & Hodgkin, S. T. 2006, MNRAS, 367, 454
Hook, I. M., McMahon, R. G., Boyle, B., & Irwin, M. J. 1994, MNRAS, 268, 305
Ivezic, Z., Tyson, J. A., Acosta, E., et al. 2008, arXiv:0805.2366
Jiang, L., Fan, X., Cool, R. J., et al. 2006, AJ, 131, 2788
Kaiser, N., Aussel, H., Burke, B. E., et al. 2002, Proc. SPIE, 4836, 154
Keller, S. C., Schmidt, B. P., Bessell, M. S., et al. 2007, PASA, 24, 1
Kong, M. Z., Wu, X.-B., Wang, R., & Han, J. L. 2006, ChJAA, 6, 396
Lawrence, A., Warren, S. J., Almaini, O., et al. 2007, MNRAS, 379, 1599
MacLeod, C. L., Brooks, K., Ivezić, Ž., et al. 2011, ApJ, 728, 26
Maddox, N., Hewett, P. C., Péroux, C., Nestor, D. B., & Wisotzki, L. 2012, MNRAS, 424, 2876
Maddox, N., Hewett, P. C., Warren, S. J., & Croom, S. M. 2008, MNRAS, 386, 1605
Markwardt, C. B. 2009, in ASP Conf. Ser. 411, Astronomical Data Analysis Software and Systems XVIII, ed. D. A. Bohlender, D. Daniel, & P. Dowler (San Francisco, CA: ASP), 251
McDonald, P., & Eisenstein, D. J. 2007, PhRvD, 76, 063009
McGreer, I. D., Helfand, D. J., & White, R. L. 2009, AJ, 138, 1925
Murray, N., Chiang, J., Grossman, S. A., & Voit, G. M. 1995, ApJ, 451, 498
Myers, A. D., Brunner, R. J., Richards, G. T., et al. 2006, ApJ, 638, 622
Oke, J. B. 1963, Natur, 197, 1040
Palanque-Delabrouille, P., Yeche, Ch., Myers, A. D., et al. 2011, A&A, 530, 122
Paris, I., Petitjean, P., Aubourg, É., et al. 2012, A&A, 548, 66
Peth, M. A., Ross, N. P., & Schneider, D. P. 2011, AJ, 141, 105
Polletta, M., Tajer, M., Maraschi, L., et al. 2007, ApJ, 663, 81
Reyes, R., Zakamska, N. L., Strauss, M. A., et al. 2010, AJ, 136, 2373
Richards, G. T., Fan, X., Newberg, H. J., et al. 2002, AJ, 123, 2945
Richards, G. T., Myers, A. D., Gray, A. G., et al. 2009, ApJS, 180, 67 (R09)
Richards, G. T., Strauss, M. A., Fan, X., et al. 2006, AJ, 131, 2766
Ross, N., Myers, A. D., Sheldon, E. S., et al. 2012, ApJS, 199, 3
Schlegel, D. J., Abdalla, F., Abraham, T., et al. 2011, arXiv:1106.1706
Schlegel, D. J., Finkbeiner, D. P., & Davis, M. 1998, ApJ, 500, 525
Schmidt, K. B., Marshall, P. J., Rix, H.-W., et al. 2010, ApJ, 714, 1194
Schmidt, M. 1963, Natur, 197, 1040
Schneider, D. P., Hall, P. B., Richards, G. T., et al. 2007, AJ, 134, 102
Schneider, D. P., Richards, G. T., Hall, P. B., et al. 2010, AJ, 139, 2360
Sesar, B., Ivezić, Ž., Lupton, R. H., et al. 2007, AJ, 134, 2236
Sharp, R. G., Sabbey, C. N., Vivas, A. K., et al. 2002, MNRAS, 337, 1153
Shen, Y., Greene, J. E., Strauss, M. A., Richards, G. T., & Schneider, D. P. 2008, ApJ, 680, 169
Shen, Y., & Liu, X. 2012, ApJ, 753, 125
Shen, Y., Richards, G. T., Strauss, M. A., et al. 2011, ApJS, 194, 45
Skrutskie, M. F., Cutri, R. M., Stiening, R., et al. 2006, AJ, 131, 1163
Smail, I., Sharp, R., Swinbank, A. M., et al. 2008, MNRAS, 389, 407
Smith, J. R., Croom, S. M., Boyle, B. J., et al. 2005, MNRAS, 359, 57
Stern, D., Assef, R. J., Benford, D. J., et al. 2012, ApJ, 753, 30
Su, D. Q., Cui, X., Wang, Y., & Yao, Z. 1998, Proc. SPIE, 3352, 76
The Dark Energy Survey Collaboration. 2005, arXiv:astro-ph/0510346
Trump, J. R., Hall, P. B., Reichard, T. A., et al. 2006, ApJS, 165, 1
Tsuzuki, Y., Kawara, K., Yoshii, Y., et al. 2006, ApJ, 650, 57
Urrutia, T., Becker, R. H., White, R. L., et al. 2009, ApJ, 698, 1095
Vanden Berk, D. E., Wilhite, B. C., Kron, R. G., et al. 2004, ApJ, 601, 692
Vestergaard, M., & Peterson, B. M. 2006, ApJ, 641, 689
Vestergaard, M., & Wilkes, B. J. 2001, ApJS, 134, 1
Warren, S. J., Hewett, P. C., & Foltz, C. B. 2000, MNRAS, 312, 827
Weinstein, M. A., Richards, G. T., Schneider, D. P., et al. 2004, ApJS, 155, 243
Weymann, R. J., Morris, S. L., Foltz, C. B., & Hewett, P. C. 1991, ApJ, 373, 23
White, M. 2003, in The Davis Meeting on Cosmic Inflation, astro-ph/0305474
White, R. L., Becker, R. H., Gregg, M. D., et al. 2000, ApJS, 126, 133
Wolf, C., Wisotzki, L., Borch, A., et al. 2003, A&A, 408, 499
Worseck, G., & Prochaska, J. X. 2011, ApJ, 728, 23
Wright, E. L., Eisenhardt, P. R. M., Mainzer, A. K., et al. 2010, AJ, 140, 1868
Wu, X.-B. 2011, NARIT Conference Series, in press (arXiv:1111.0738)
Wu, X.-B., Chen, Z.-Y., Jia, Z.-D., et al. 2010a, RAA, 10, 737
Wu, X.-B., Hao, G., Jia, Z., Zhang, Y., & Peng, N. 2012, AJ, 144, 49
Wu, X.-B., & Jia, Z. 2010, MNRAS, 406, 1583
Wu, X.-B., Jia, Z.-D., Chen, Z.-Y., et al. 2010b, RAA, 10, 745
Wu, X.-B., Wang, R., Schmidt, K. B., et al. 2011, AJ, 142, 78
Wu, X.-B., Zhang, W., & Zhou, X. 2004, ChJAA, 4, 17
Yan, L., Donoso, E., Tsai, C.-W., et al. 2013, AJ, 145, 55
York, D. G., Adelman, J., Anderson, J. E., Jr., et al. 2000, AJ, 120, 1579
Zhao, G., Zhao, Y.-H., Chu, Y.-Q., Jing, Y.-P., & Deng, L.-C. 2012, RAA, 12, 723
Zuo, W., Wu, X.-B., Liu, Y.-Q., & Jiao, C.-L. 2012, ApJ, 758, 104